7.0T nuclear magnetic resonance evaluation of the amyloid beta (1–40) animal model of Alzheimer's disease: comparison of cytology verification

Lei Zhang[1], Shuai Dong[2], Guixiang Zhao[3], Yu Ma[4]

1 MR Neuroradiology Room, Beijing Tiantan Hospital Affiliated to Capital Medical University, Beijing, China
2 Department of Neurology, Sixth People's Hospital of Jinan, Jinan, Shandong Province, China
3 Department of Rehabilitation Medicine, Sixth People's Hospital of Jinan, Jinan, Shandong Province, China
4 Tsinghua University Yuquan Hospital, Beijing, China

Corresponding author:
Yu Ma, M.D., Tsinghua University Yuquan Hospital, Beijing 100049, China, lymayu@163. com.

Abstract

3.0T magnetic resonance spectroscopic imaging is a commonly used method in the research of brain function in Alzheimer's disease. However, the role of 7.0T high-field magnetic resonance spectroscopic imaging in brain function of Alzheimer's disease remains unclear. In this study, 7.0T magnetic resonance spectroscopy showed that in the hippocampus of Alzheimer's disease rats, the N-acetylaspartate wave crest was reduced, and the creatine and choline wave crest was elevated. This finding was further supported by hematoxylin-eosin staining, which showed a loss of hippocampal neurons and more glial cells. Moreover, electron microscopy showed neuronal shrinkage and mitochondrial rupture, and scanning electron microscopy revealed small size hippocampal synaptic vesicles, incomplete synaptic structure, and reduced number. Overall, the results revealed that 7.0T high-field nuclear magnetic resonance spectroscopy detected the lesions and functional changes in hippocampal neurons of Alzheimer's disease rats *in vivo*, allowing the possibility for assessing the success rate and grading of the amyloid beta (1–40) animal model of Alzheimer's disease.

Key Words: nerve regeneration; Alzheimer's disease; Aβ1–40; high-field functional magnetic resonance; nuclear magnetic resonance spectroscopy; neuropathology; N-acetylaspartate; creatine; choline; hippocampus; NSFC grant; neural regeneration

Zhang L, Dong S, Zhao GX, Ma Y. 7.0T nuclear magnetic resonance evaluation of the amyloid beta (1–40) animal model of Alzheimer's disease: comparison of cytology verification. Neural Regen Res. 2014;9(4):430-435.

Introduction

No accepted biomarker for Alzheimer's disease exists, and this disease can only by diagnosed by brain biopsy or autopsy clinics[1-3]. The key issue in the current study was to improve the accuracy of clinical diagnosis of Alzheimer's disease and to improve the sensitivity of early diagnosis of this disease. Changes in the metabolism of brain tissue at the molecular level are a sensitive indicator of brain function and disease lesions. Magnetic resonance spectroscopy can quantitatively analyze *in vivo* abnormalities of biochemical metabolism within brain tissue, thus allowing for a better understanding of the pathophysiology of Alzheimer's disease[4-5]. This technology has been applied in *in vivo* studies since the end of the 20th century[6], but its clinical application is limited due to low resolution of low-field nuclear magnetic resonance imaging (MRI)[7]. High-field nuclear magnetic resonance allows great development of this technology because it clearly shows the microscopic anatomical structure of the entorhinal cortex and hippocampus with a relative objective due to external factors not affecting this technique. Compared with

3.0T magnetic resonance spectroscopy, high-field magnetic resonance spectroscopy (≥ 7.0T) exhibits high spatial resolution and density resolution, microscopic imaging of the living body, and obtains both high scanning resolution and result precision within a shorter scan time, thus providing a higher value in clinical diagnosis. However, high-field nuclear magnetic resonance spectroscopy is poorly understood due to its cost and conditions[8-14], and its application in animal models of Alzheimer's disease has been rarely reported.

Alzheimer's disease is characterized by progressive cognitive and behavioral impairment[15]. One of the major neuropathological hallmarks of Alzheimer's disease is the accumulation of β-amyloid (Aβ) peptide[16]. Aβ1–40 may allow for this species to diffuse to larger distances resulting in an increased deposition around brain vessels[17]. Amyloid precursor protein[16], presenilin 1[18] and presenilin 2 genes[19-20] have been identified to cause familial Alzheimer's disease. All of these mutations lead to abnormal accumulation of Aβ, supporting a significant role of Aβ in Alzheimer's disease. Several studies have shown that acute or chronic adminis-

Table 1 Escape latency, number of platform quadrant crossings, and time spent in the quadrant in the Morris water maze task of Alzheimer's disease rats and control rats

| Group | Escape latency (second) | | | | | Number of crossing platform quadrant (time/2 minutes) | Dwell time (second) |
	Day 1	Day 2	Day 3	Day 4	Day 5		
Model	58.3±26.6	51.35±17.0[a]	46.6±27.8[a]	38.6±17.2[a]	30.2±15.7[a]	3.4±1.1[a]	9.4±2.1[a]
Control	51.2±20.2	19.7±11.2	13.5±7.6	9.8±6.5	8.8±4.6	8.7±2.9	28.2±2.8

Data are expressed as mean ± SD and the differences between groups were compared using the independent sample *t*-test. [a]$P < 0.05$, *vs*. control group.

Table 2 Changes of N-acetylaspartate/creatine, N-acetylaspartate/choline, and choline/creatine ratios in brains of Alzheimer's disease rats and control rats

Group	N-acetylaspartate/creatine	N-acetylaspartate/choline	Choline/creatine
Model	1.37±0.15[a]	1.33±0.17[a]	0.91±0.12
Control	1.46±0.21	1.39±0.13	0.87±0.09

Data are expressed as mean ± SD and the differences between groups were compared using the independent sample *t*-test. [a]$P < 0.05$, *vs*. control group.
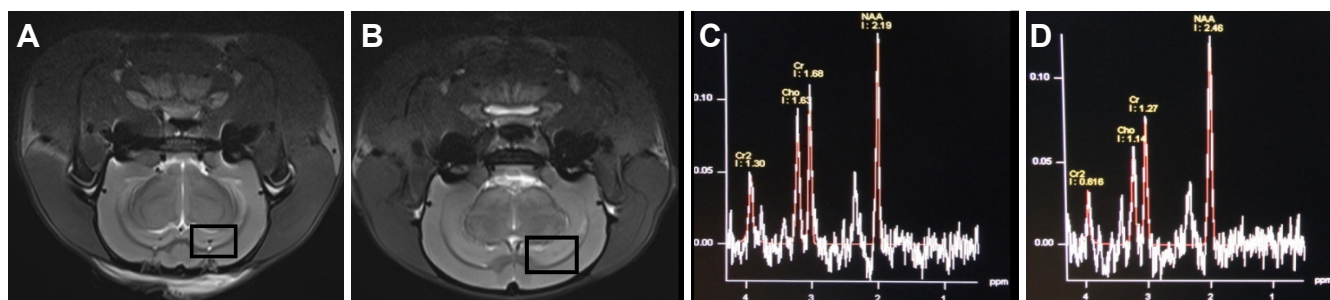
Figure 1 7.0T high-field magnetic resonance spectroscopy images of Alzheimer's disease rats.
The MRI T2-weighted images between rats 2 weeks after Alzheimer's disease was induced (A) and controls (B) were not significantly different. The panels represent magnetic resonance spectroscopy sensitive areas. (C) Magnetic resonance spectroscopy in the hippocampus of rats 2 weeks after Alzheimer's disease was performed. The N-acetylaspartate (NAA), choline (Cho), and creatine (Cr) peaks were 2.19, 1.63, and 1.68 ppm, respectively. (D) Magnetic resonance spectroscopy in the hippocampus of control rats. The NAA, Cho, and Cr peaks were 2.46, 1.14, and 1.27 ppm, respectively.

tration of Aβ into the brain causes some pathological events observed in Alzheimer's disease[21-22]. The aim of the present study was to characterize the early functional changes and pathological detections in the hippocampus of Alzheimer's disease rats. We established rat models of Alzheimer's disease using a stereotactic microinjection of Aβ1–40 into the bilateral CA1 hippocampal region. The brain was scanned by high-field 7.0T magnetic resonance spectroscopy.

Results
Quantitative analysis of experimental animals
Thirty rats were randomly divided into the model group and control group. In the model group, rats were injected with Aβ1–40 into the bilateral CA1 hippocampal region to establish Alzheimer's disease-like pathology. All rats involved were used for analysis.
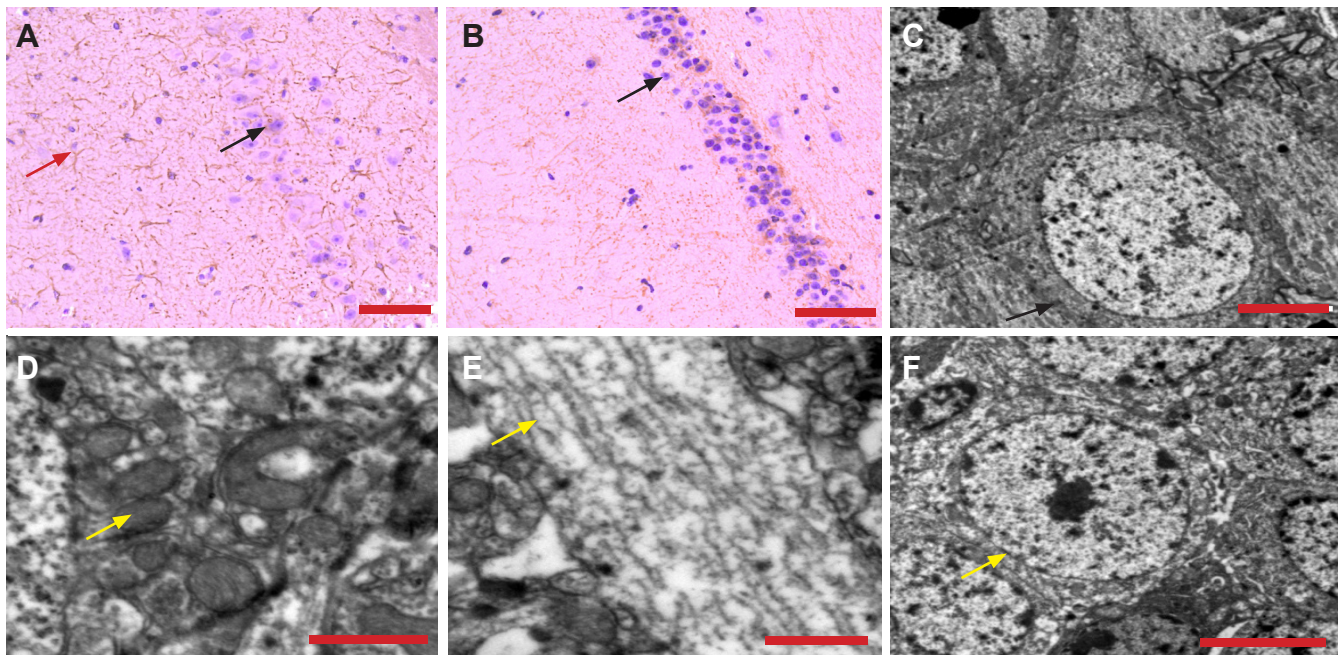
Behavioral changes in Alzheimer's disease rats
On day 1 of the place navigation test in the Morris water maze task, no significant difference in the escape latency between the rat model of Alzheimer's disease and normal rats was found. On the second day, the escape latency of Alzheimer's disease rats was significantly ($P < 0.05$) longer than normal rats (Table 1). In the spatial exploration test, the number of platform quadrant crossings in the Alzheimer's disease group was significantly ($P < 0.05$) reduced and the time spent in the quandrant was also significantly ($P < 0.05$) shortened compared with the control group (Table 1).

7.0T high-field magnetic resonance spectroscopy imaging of Alzheimer's disease rats
Two weeks after inducing Alzheimer's disease, T1WI and T2WI signals of MRI showed no apparent change in the bilateral hippocampi of Alzheimer's disease rats (Figure 1A, B). Magnetic resonance spectroscopy showed that the N-acetylaspartate peak was reduced and the creatine and choline peaks were elevated in the model group compared with the control group (Figure 1C, D). The N-acetylaspartate/cre-

Figure 2 Hematoxylin-eosin staining of the pathological changes and transmission electron microscopy of the ultrastructural changes in the hippocampus of Alzheimer's disease rats.
(A) Disordered structure and neuronal loss (black arrow), and increased glia (red arrow) in the hippocampal CA1 region of Alzheimer's disease rats. (B) Normal morphology of hippocampal CA1 neurons (arrow) in control rats. In Alzheimer's disease rats, hippocampal neurons were condensed (C, arrow), mitochondrial structure disorderly arranged (D, arrow), microtubular structures, which were chaotic (discontinuous and ruptured) (E, arrow). The microstructure of hippocampal neurons in the control group was normal (F, arrow). Scale bar: 50 μm (A, B), 5 μm (C, F), and 1 μm (D, E).

atine and N-acetylaspartate/choline ratios were significantly ($P < 0.05$) reduced, but choline/creatine ratios remained unchanged (Table 2).

Pathological changes in the hippocampus of Alzheimer's disease rats
Hematoxylin-eosin staining showed a loss of hippocampal neurons in Alzheimer's disease rats compared with controls (Figure 2A). Furthermore, hippocampal CA1 neurons were disorderly arranged, cell morphology was abnormal, and more astrocytes and microglia were observed, compared with the control group (Figure 2B).

Cell counts were 13 ± 6 neurons/100 μm^2 and 25 ± 8 glial cells/100 μm^2 in the CA1 region of the hippocampus in the Alzheimer's disease group, and 27 ± 8 neurons/100 μm^2 and 10 ± 5 glial cells/100 μm^2 in the same region of the control group.

Ultrastructural changes in the hippocampus of Alzheimer's disease rats
Transmission electron microscopy showed that normal morphology of hippocampal CA1 neurons in control rats (Figure 2F). Furthermore, these rats exhibited an intact neuronal structure. We also observed the cytoplasm, nucleus, nucleolus, normal organelles (mitochondria and Golgi body), normal blood capillary, endothelial cells, pericytes, the presynaptic membrane, and the postsynaptic membrane. Excitatory neurotransmitter (round, clear vesicles) and inhibitory neurotransmitter (slightly large size, sheath) were also observed. In the Alzheimer's disease group, hippocam-

pal neurons and nuclear substances were condensed and aggregated, secondary lysosomes were increased, the Golgi body structure was unclear, lipofuscin was deposited, the mitochondrial structure was disorderly arranged, and microtubules were discontinuous and ruptured (Figure 2C–E). Furthermore, the synapse was edemic, presynaptic excitatory neurotransmitter vesicles were increased, the astrocytic cytoplasm was mildly swollen, and astrocytes were increased.

Discussion
Nuclear magnetic resonance spectroscopy analyzes brain metabolites, such as N-acetylaspartate, creatine, choline, myo-inositol, and lactate. N-acetylaspartate is mainly distributed in neurons and is considered to be one of the numerous neuronal markers used in magnetic resonance spectroscopy[23-24]. N-acetylaspartate also reflects mitochondrial function. The concentration of N-acetylaspartate is an indicator of the number of neurons and neuronal metabolism. A reduced level of N-acetylaspartate reflects neuronal loss, as well as functional abnormalities[25]. In the present study, the peak value of hippocampal N-acetylaspartate 2 weeks after inducing Alzheimer's disease to rats was significantly lower than the control group. This result indicated that injection of Aβ1–40 may have caused hippocampal neuronal loss or functional impairment. Creatine, including creatine phosphate, provides a reserve of high-energy phosphate and buffers the conversion of ATP to ADP, and is thus considered a sign of energy metabolism. Creatine concentration is stable in both physiological and pathological conditions, and is often used as a reference to calculate the relative concentration

of other metabolites[26]. We adopted creatine as an internal reference to observe changes in the concentration of other metabolites. Brain damage incurred by Alzheimer's disease mainly occurs within the gray matter and is characterized by neuronal loss. Magnetic resonance spectroscopy has shown that the N-acetylaspartate/creatine ratio in the majority of Alzheimer's disease patients is lower than that of the normal (control) group[27-30]. The present study supported these previous results, showing a significantly higher N-acetylaspartate/creatine ratio in the hippocampus of Alzheimer's disease rats compared with the control group. However, other studies have shown no significant difference[31-34]. Choline belongs to the cholinergic phosphate family, and is a component of cell membranes which is involved in phospholipid synthesis and metabolism, as well as myelin formation. The variation in levels of choline reflects changes in the number of glial cells[6]. Choline and creatine are generated from glial cells, and increased levels of the two indicate glial cell proliferation[6]. The present study showed a higher choline peak in the hippocampus of Alzheimer's disease rats compared with normal rats, suggesting the proliferation of glial cells in the hippocampus. Furthermore, the N-acetylaspartate/choline ratio was significantly reduced compared with the control group, which supports the previous study[32]. Although magnetic resonance spectroscopy is rarely applied for rat models of Alzheimer's disease, its use in Alzheimer's disease patients has revealed an elevation in the choline/creatine ratio in this group[32]. These differences may be explained by the variation of the detection site or the severity of the disease, and the elevated ratio has been proposed to be closely linked with the degeneration of neuronal membranes[35]. The decline of hippocampal N-acetylaspartate/creatine ratio is mediated by the loss of hippocampal neurons, the formation of senile plaques, and neurofibrillary tangles[32]. Hematoxylin-eosin staining in the present study revealed the loss of hippocampal neurons and more glial cells. In addition, electron microscopy results showed neuronal shrinkage and mitochondrial rupture. These findings were consistent with magnetic resonance spectroscopy results, showing the reduced N-acetylaspartate peak, and the elevated creatine and choline peaks. Furthermore, Alzheimer's disease rats had memory loss and decline of learning capacity. Overall, these characteristics were similar to the pathology and behavioral deficits of Alzheimer's disease patients. These experimental findings indicated that nuclear magnetic resonance spectroscopy effectively detected the lesions and functional changes in the hippocampus of Alzheimer's disease rats *in vivo*. Therefore, this technique may allow the possibility of evaluating the success rate of an Alzheimer's disease model in determining a treatment strategy for this disease.

In the present study, a rat model of Alzheimer's disease was established 2 weeks after microinjection of Aβ1–40 into the bilateral hippocampi. Moreover, nuclear magnetic resonance spectroscopy results were consistent with the behavioral and neuropathological changes of Alzheimer's disease. Although we only reported on preliminary applications of 7.0T high-field magnetic resonance spectroscopy 2 weeks after inducing Alzheimer's disease, our findings showed that this technique is a non-invasive method of possibly diagnosing this disease.

Materials and Methods

Design
A randomized controlled animal study.

Time and setting
Experiments were performed from January 2012 to August 2012 in Beijing Neurosurgical Institute, Beijing, China.

Materials
Animals
Thirty Wistar male rats (260–280 g) of clean grade were provided by Experimental Animal Center of the Zoology Department, Chinese Academy of Military Medical Sciences (license No. SCXK (Army) 2007-004). Animals were housed at 22°C under 60–70% humidity, on a 12-hour light/dark cycle, with *ad libitum* access to food and water. Experiments were performed under strict accordance with the *Guidance Suggestions for the Care and Use of Laboratory Animals*, issued by the Ministry of Science and Technology of China[36], and approval was obtained from the Animal Ethics Committee of Beijing Neurosurgical Institute Affiliated to Capital Medical University (2012011012).

Drugs
Aβ1–40 was purchased from Sigma-Aldrich (St. Louis, MO, USA). Aβ1–40 (1 mg) was dissolved in sterile saline at 1 g/L and incubated at 37°C in the water bath for 7 days to obtain aggregated Aβ1–40.

Methods
Establishment of the Alzheimer's disease model
Rats were anesthetized with 10% chloral hydrate (300 mg/kg) *via* intraperitoneal injection and placed in a stereotactic apparatus (David Kopf, Tujunga, CA, USA). After the hair was sheared and the skin was disinfected, a longitudinal incision was made in the middle of the dorsal skull, the subcutaneous tissue was cut, and the osseous fascia was bluntly isolated. According to the Rat Brain in Stereotactic Coordinates[37], the coordinates of the bilateral hippocampal CA1 regions were determined (3.3 mm posterior to bregma, 2 mm lateral to the midline, 2.7 mm inferior to the dura mater). The skull around the CA1 region was drilled using a small dental drill and the vertical position of the microsyringe was corrected. Aβ1–40 and (8 μL) was then injected for 10 minutes and the needle was maintained for 10 minutes. The needle was subsequently pulled out slowly, the wound sutured, and the rats were returned to the cage. After surgery, the rats were intramuscularly injected with 16×10^4 U penicillin for 3 days to prevent infection. The control group was given 5 μL saline.

Morris water maze task
The Morris water maze (Chinese Academy of Medical Science, Beijing, China) consisted of a circular water tank (diameter 150 cm; height 50 cm) filled with water, which was maintained at 25 ± 1°C in a suitably equipped room at a constant temperature of 24 ± 1°C and humidity. By using two fictitious vertical lines, the tank was divided into four

imaginary quadrants of equal sizes (designated as quadrants I, II, III, IV) with the escape platform located in quadrant III relative to the spatial cues for all training trials. The escape platform (diameter 10 cm; height 24 cm) was round and black, located 30 cm from the wall of the water tank. The surface of the escape platform was submerged 1 cm below the water surface. The experiment was performed for 6 days, including the placed navigation test and spatial exploration test. On day 9 after Alzheimer's disease induction, the place navigation test was performed. Four trials where performed for each rat daily for 5 days and always faced the wall of water tank when they were carefully placed into the maze with four different starting positions. The time taken to find the platform was recorded as the escape latency. If a rat failed to find the platform within 120 seconds, this latency was recorded as 120 seconds, and the rat was allowed to take a rest on the platform for 30 seconds before continuing to the next trial. On day 14, we performed a spatial exploration test, recording the times the rats crossed the target platform quadrant. The period of retention in the target platform quadrant within 120 seconds reflected the spatial memory capacity of experimental rats.

MRI and magnetic resonance spectroscopy

The Bruker 7.0T MRI equipment (Bruker Medical Systems, CLinScan, Berlin, Germany) was used 2 weeks after Alzheimer's disease establishment. MRI parameters included: T1WI repetition time = 2,000 ms, T1WI echo time = 38 ms, T2WI repetition time = 3,140 ms, T2WI echo time = 37 ms, field of view = 40 mm × 40 mm, matrix = 240 × 320, and slice thickness = 1 mm. Magnetic resonance spectroscopy parameters included: multi-voxel spectroscopy scanning, including the hippocampus and temporal lobe, T2WI repetition time = 3,140 ms, T2WI echo time = 37 ms, field of view = 40 mm × 40 mm, matrix = 240 × 320, slice thickness = 1 mm, and scan time = 217 seconds. The N-acetylaspartate, creatine, and choline contents were detected with magnetic resonance spectroscopy.

Hematoxylin-eosin staining

Two weeks after Alzheimer's disease induction, rats were killed under anesthesia and perfused *via* the left ventricle with saline and 0.1 mol/L phosphate buffer (pH 7.2) containing 4% paraformaldehyde. After perfusion, the right atrial appendage was cut and the hippocampus removed and fixed for 24 hours. Coronal slices (30 μm) were incubated at 60°C for 30 minutes, dewaxed in xylene, and rehydrated in gradient ethanol. The slices were subsequently stained with hematoxylin for over 10 minutes and differentiated with 1% hydrochloric acid in ethanol for 2–3 seconds. Differentiation was terminated using tap water. Then slices were counterstained with eosin for 5 minutes, dehydrated in gradient ethanol, placed in xylene, and mounted. Slices were observed under the XSP8CE optical microscope (Shanghai Changfang Optical Instrument Co., Ltd., Shanghai, China).

Electron microscopy

Two weeks after Alzheimer's disease induction, rats were killed under anesthesia and the brain harvested. The hippo-campus was fixed in 2% paraformaldehyde and 2.5% glutaraldehyde at 4°C for 2 hours, rinsed with sodium dimethylarsenate buffer (pH 7.2), and fixed in 1% osmium tetroxide for 2 hours. The tissue was incubated with 100% ethanol followed by propylene oxide and resin (1:4) at room temperature for 1 hour then soaked in pure resin for 2 hours and embedded in Epon812. Slices were then cut into 1 μm semi-thin sections for Giemsa-methylene blue staining to view under the optical microscope. Sections were subsequently stained with uranyl acetate and lead citrate and observed under transmission electron microscope (Hitachi-7650; Hitachi, Tokyo, Japan).

Statistical analysis

All data are expressed as mean ± SD. All data were analyzed using SPSS 13.0 software (SPSS, Chicago, IL, USA). The difference between the groups was compared using an independent sample *t*-test. $P \leq 0.05$ was considered statistically significant.

Author contributions: *Ma Y was responsible for the study design. Zhang L and Dong S implemented the experiment. Zhang L and Zhao GX evaluated the experiment. Zhang L collected data and wrote the manuscript. Ma Y was responsible for the article. All authors approved the final version of the manuscript.*
Conflicts of interest: *None declared.*
Peer review: *In this study, we investigated biological characteristics of animal models of Alzheimer's disease and the correlation of the brain imaging of biological, behavioral and pathological changes in Alzheimer's disease rats, through 7.0T high-field functional magnetic resonance imaging evaluation. The results showed that 7.0T high-field functional magnetic resonance imaging is a non-invasive detection method in Alzheimer's disease.*

References

[1] Dalvi A. Alzheimer's disease. Dis Mon. 2012;58:666-677.

[2] Zhang ZQ, Zahner GE, Roman GC, et al. Studies on the prevalence of subtype of dementia in Beijing, Xi'an, Shanghai and Chengdu. Zhongguo Xiandai Shenjing Jibing Zazhi. 2005;5:156-157.

[3] Wang Y, Chai Y. Summarize on the studies of social influence factors on Alzheimer's disease. Zhongguo Shehui Yixue Zazhi. 2012;29:50-51.

[4] Zhang Y, Xu Y, Nie H, et al. Prevalence of dementia and major dementia subtypes in the Chinese populations: a meta-analysis of dementia prevalence surveys, 1980-2010. J Clin Neurosci. 2012;19:1333-1337.

[5] Hall H, Cuellar-Baena S, Dahlberg C, et al. Magnetic resonance spectroscopic methods for the assessment of metabolic functions in the diseased brain. Curr Top Behav Neurosci. 2012;11:169-198.

[6] Rae C. RE: Magnetic resonance spectroscopy of the brain: review of metabolites and clinical applications. Clin Radiol. 2009;64:1042-1043.

[7] Soares DP, Law M. Magnetic resonance spectroscopy of the brain: review of metabolites and clinical applications. Clin Radiol. 2009; 64:12-21.

[8] Currie S, Hadjivassiliou M, Craven IJ, et al. Magnetic resonance spectroscopy of the brain. Postgrad Med J. 2013;89:94-106.

[9] Gordon ML, Kingsley PB, Goldberg TE, et al. An open-label exploratory study with memantine: correlation between proton magnetic resonance spectroscopy and cognition in patients with mild to moderate Alzheimer's disease. Dement Geriatr Cogn Dis Extra. 2012;2:312-320.

[10] Henry MS, Passmore AP, Todd S, et al. The development of effective biomarkers for Alzheimer's disease: a review. Int J Geriatr Psychiatry. 2013;28:331-340.

[11] Silveira de Souza A, de Oliveira-Souza R, Moll J, et al. Contribution of 1H spectroscopy to a brief cognitive-functional test battery for the diagnosis of mild Alzheimer's disease. Dement Geriatr Cogn Disord. 2011;32:351-361.

[12] Román G, Pascual B. Contribution of neuroimaging to the diagnosis of Alzheimer's disease and vascular dementia. Arch Med Res. 2012;43:671-676.

[13] Gordon ML, Kingsley PB, Goldberg TE, et al. An open-label exploratory study with memantine: correlation between proton magnetic resonance spectroscopy and cognition in patients with mild to moderate Alzheimer's disease. Dement Geriatr Cogn Dis Extra. 2012;2:312-320.

[14] Warsi MA, Molloy W, Noseworthy MD. Correlating brain blood oxygenation level dependent (BOLD) fractal dimension mapping with magnetic resonance spectroscopy (MRS) in Alzheimer's disease. MAGMA. 2012;25:335-344.

[15] Dong XH, Chai XQ. Alzheimer's disease transgenic animal models: How to get more similar pathological characteristics? Zhongguo Zuzhi Gongcheng Yanjiu. 2013;17:8075-8082.

[16] Glenner GG, Wong CW. Alzheimer's disease: initial report of the purification and characterization of a novel cerebrovascular amyloid protein. 1984. Biochem Biophys Res Commun. 2012;425:534-539.

[17] Goate A. Segregation of a missense mutation in the amyloid beta-protein precursor gene with familial Alzheimer's disease. J Alzheimers Dis. 2006;9:341-347.

[18] Sherrington R, Rogaev EI, Liang Y, et al. Cloning of a gene bearing missense mutations in early-onset familial Alzheimer's disease. Nature. 1995;375:754-760.

[19] Levy-Lahad E, Wasco W, Poorkaj P, et al. Candidate gene for the chromosome 1 familial Alzheimer's disease locus. Science. 1995;269:973-977.

[20] Rogaev EI, Sherrington R, Rogaeva EA, et al. Familial Alzheimer's disease in kindreds with missense mutations in a gene on chromosome 1 related to the Alzheimer's disease type 3 gene. Nature. 1995;376:775-778.

[21] Yamaguchi Y, Miyashita H, Tsunekawa H, et al. Effects of a novel cognitive enhancer, spiro[imidazo-[1,2-a]pyridine-3,2-indan]-2(3H)-one (ZSET1446), on learning impairments induced by amyloid-beta1-40 in the rat. J Pharmacol Exp Ther. 2006;317:1079-1087.

[22] Van Dam D, De Deyn PP. Drug discovery in dementia: the role of rodent models. Nat Rev Drug Discov. 2006;5:956-970.

[23] Martin WR. MR spectroscopy in neurodegenerative disease. Mol Imaging Biol. 2007;9:196-203.

[24] McGeer PL, Kamo H, Harrop R, et al. Comparison of PET, MRI, and CT with pathology in a proven case of Alzheimer's disease. Neurology. 1986;36:1569-1574.

[25] Chen JG, Charles HC, Barboriak DP, et al. Magnetic resonance spectroscopy in Alzheimer's disease: focus on N-acetylaspartate. Acta Neurol Scand Suppl. 2000;176:20-26.

[26] Jessen F, Block W, Träber F, et al. Proton MR spectroscopy detects a relative decrease of N-acetylaspartate in the medial temporal lobe of patients with AD. Neurology. 2000;55:684-688.

[27] Shiino A, Matsuda M, Morikawa S, et al. Proton magnetic resonance spectroscopy with dementia. Surg Neurol. 1993;39:143-147.

[28] Sun YA, He XB, Miao CC, et al. Magnetic resonance spectroscopy in evaluating hippocampus changes of patients with mild cognitive impairment. Zhongguo Zuzhi Gongcheng Yanjiu yu Linchuang Kangfu. 2009;13:5098-5103.

[29] Franczak M, Prost RW, Antuono PG, et al. Proton magnetic resonance spectroscopy of the hippocampus in patients with mild cognitive impairment: a pilot study. J Comput Assist Tomogr. 2007;31:666-670.

[30] Yang GY, Gao MY, Liang XM, et al. Clinical application of 3.0T proton magnetic resonance spectroscopy in Alzheimer's disease. Guangdong Yixueyuan Xuebao. 2009;27:26-28.

[31] Murphy DG, Bottomley PA, Salerno JA, et al. An in vivo study of phosphorus and glucose metabolism in Alzheimer's disease using magnetic resonance spectroscopy and PET. Arch Gen Psychiatry. 1993;50:341-349.

[32] Huang W, Alexander GE, Chang L, et al. Brain metabolite concentration and dementia severity in Alzheimer's disease: a (1)H MRS study. Neurology. 2001;57:626-632.

[33] Ernst T, Chang L, Melchor R, et al. Frontotemporal dementia and early Alzheimer disease: differentiation with frontal lobe H-1 MR spectroscopy. Radiology. 1997;203:829-836.

[34] Li YH, Zhang ZY, Yin SL. Proton MR spectroscopy study of posterior portion cingulate gyrus both in patients with Alzheimer's disease and normal adults. Zhongguo Yixue Yingxiang Jishu. 2006;22:64-66.

[35] Chantal S, Braun CM, Bouchard RW, et al. Similar 1H magnetic resonance spectroscopic metabolic pattern in the medial temporal lobes of patients with mild cognitive impairment and Alzheimer disease. Brain Res. 2004;1003:26-35.

[36] The Ministry of Science and Technology of the People's Republic of China. Guidance Suggestions for the Care and Use of Laboratory Animals. 2006-09-30.

[37] Paxinos G, Watson C. The Rat Brain in Stereotaxic Coordinates. Sydney: Academic Press. 1998.